Thermally Induced Endo/Exo Isomerization of Polyimides. An AM1 Study Using Nadimide as a Model for the Reactive End-Caps of PMR Prepolymers

P. Iratcabal*,† and H. Cardy‡

Université de Pau et des Pays de l'Adour, Centre Universitaire de Recherche Scientifique, Laboratoire de Physicochimie des Polymères, URA 1494, Avenue de l'Université, 64000 PAU, France, and Université de Pau et des Pays de l'Adour, Laboratoire de Chimie Structurale, URA 474, Institut de Formation et de Recherche, Rue Jules Ferry, 64000 PAU, France

Received April 18, 1995®

This paper provides an AM1-HE-SDCI approach to the thermal properties of nadimide. To gauge the ability of this formalism to reproduce experimental data, three prototype Diels–Alder reactions, butadiene + ethylene, cyclopentadiene + ethylene, and cyclopentadiene + acrolein, have been revisited. On the basis of these tests it is concluded that the AM1-HE-SDCI procedure can handle both the synchronous concerted and stepwise processes in Diels–Alder reactions. It appears particularly well suited for modeling the decomposition of Diels–Alder adducts. With respect to the conversion of *endo*-nadimide to its exo isomer, external (i.e. completely dissociative) and internal (i.e. partially dissociative) pathways are predicted to be nearly competitive. The nonconcerted stepwise isomerization process involves the intermediacy of a conformationally mobile biradical species that can undergo intramolecular hydrogen atom transfer to lead directly to the exo adduct without retrogression to the addends. These results bear a strong indication that homopolymerization of the norbornene rings in low molecular weight nadimide end-capped polyimides can be reasonably modeled with the participation of biradical intermediates. The origins of the sensitivity of rates to changes in the nature of the reaction medium have been sought in solvation and internal pressure effects.

Introduction

The study of the thermal behavior of low molecular weight nadimide end-capped polyimides has received a considerable attention over the past 25 years.[1-8] Such unsaturated oligomers polymerize under thermal activation to form thermostable resins with high mechanical properties for applications in aerospace and electronic industries. Structures and hence, properties, of these crosslinked oligomers are strongly dependent on the cure processes, which are usually based on empirical observation. Any mechanistic information from theory or experiment toward a better understanding of the homopolymerization should be helpful to carry out polymer synthesis in a structurally selective manner and without producing volatiles.

In order to learn more about the mechanisms of polymerization operative, *N*-phenylnadimide has been often used to model the chemical reactivity of the nadimide end-caps.[2-4] The terminal norbornene rings were found to undergo two kinds of chemical processes depending on the cure temperature: (i) the usual monomer endo/exo isomerization,[9-15] (ii) polymerization. Whereas isomerization is predominant at $T \leq 200$ °C, both processes compete in the higher temperature domain.

† Laboratoire de Physicochimie des Polymères.

‡ Laboratoire de Chimie Structurale.

® Abstract published in *Advance ACS Abstracts,* September 15, 1995.

(1) (a) Serafini, T. T. *PMR Polyimides-Review and Update* (NASA, 1982), NASA TM-82821. (b) Jones, R. J.; Vaughan, R. W.; Burns, E. A. *Thermally Stable Laminating Resins*, TRW-16402-6012-RO-00, NASA CR-72984 (TRW Systems Group, 1972).

(2) (a) Gaylord, N. G.; Martan, M. *Polym. Prepr.* **1980**, *22*, 11. (b) Wong, A. C.; Ritchey, W. M. *Spectrosc. Lett.* **1980**, *13*, 503. (c) Wong, A. C.; Ritchey, W. M. *Macromolecules* **1981**, *14*, 825.

(3) (a) Vijayakumar, C. T.; Lederer, K. *J. Polym. Sci. Part. A: Polym. Chem.* **1989**, *27*, 1. (b) Hay, J. N.; Boyle, J. D.; Parker, S. F.; Wilson, D. *Polymer* **1989**, *30*, 1032. (c) Sukenik, C. N.; Malhotra, V.; Varde, U. *Reactive Oligomers*; Harris, F. W., Spinnelli, H. J., Eds.; ACS Symposium Series 282, 1985; p 53.

(4) Dong, W.; Zhitang, H. *Gaofenzi Tongxun* **1981**, *3*, 212.

(5) (a) Scola, D. A.; Stevens, M. P. *J. Appl. Polym. Sci.* **1981**, *26*, 231. (b) Scola, D. A.; Pater, R. H. *Polym. Prep. Am. Chem. Soc. Div. Polym. Chem.* **1979**, *20(2)*, 564. (c) Odagiri, N.; Yamashita, T.; Tobukuro, K. In *Composites S6: Recent Advances in Japan and United States*; Kawata, K., Umekawa, S., Kobayashi, A., Eds.; Proc Japan US. CCM-III, Tokyo, 53 (1986). (d) Wilson, D.; Wells, J. K.; Lind, D.; Owens, G. A.; Johnson, F. *SAMPE J.*, May, June, 35 (1987).

(6) Serafini, T. T.; Delvigs, P. *Appl. Polym. Symp.* **1973**, *22*, 89.

(7) (a) Dokoshi, N. *Kobunshi* **1974**, *23*, 125. (b) Dynes, P. J.; Panos, R. M.; Hamermesh, C. L. *J. Appl. Polym. Sci.* **1980**, *25*, 1059.

(8) Patel, R. D.; Patel, M. R.; Bhardwaj, I. S.*Thermochim. Acta* **1981**, *48*, 11.

(9) (a) Baldwin, J. E. *J. Org. Chem.* **1966**, *31*, 2441. (b) Mironov, V. A.; Fadeeva, T. M.; Stepaniantz, A. U.; Akhrem, A. A. *Tetrahedron Lett.* **1966**, *47*, 5823. (c) Canter, C.; Scheidegger, U.; Roberts, J. D. *J. Am. Chem. Soc.* **1965**, *87*, 2771. (d) Herndon, W. C.; Grayson, C. R.; Manion, J. M. *J. Org. Chem.* **1967**, *32*, 526.

(10) (a) Baldwin, J. E.; Roberts, J. D. *J. Am. Chem. Soc.* **1963**, *85*, 115. (b) Berson, J. A.; Reynolds, R. D. *J. Am. Chem. Soc.* **1955**, *77*, 4434. (c) Berson, J. A.; Reynolds, R. D.; Jones, W. M. *J. Am. Chem. Soc.* **1956**, *78*, 6049. (d) Berson, J. A.; Mueller, W. A. *J. Am. Chem. Soc.* **1961**, *83*, 4940. (e) Craig, D. *J. Am. Chem. Soc.* **1951**, *73*, 4889.

(11) (a) Berson, J. A.; Swidler, R. *J. Am. Chem. Soc.* **1953**, *75*, 1721. (b) Craig, D.; Shipman, J. J.; Kiehl, J.; Widmer, F.; Fowler, R.; Hawthorne, A. *J. Am. Chem. Soc.* **1954**, *76*, 4573. (c) Kwart, H.; Burchuk, I. *J. Am. Chem. Soc.* **1952**, *74*, 3094. (d) Lee, M. W.; Herndon, W. C. *J. Org. Chem.* **1978**, *43*, 518. (e) Anet, F. A. L. *Tetrahedron Lett.* **1962**, *25*, 1219. (f) Woodward, R. B.; Baer, H. *J. Am. Chem. Soc.* **1944**, *66*, 645.

(12) Seltzer, S. *J. Am. Chem. Soc.* **1965**, *87*, 1534.

(13) (a) Kwart, H.; King, K. *Chem. Rev.* **1968**, *68*, 415. (b) Martin, J. G.; Hill, R. K. *Chem. Rev.* **1961**, *61*, 537. (c) Oppolzer, W. *Angew. Chem., Int. Ed. Engl.* **1984**, *23*, 876. (d) Ripoll, J. L.; Rouessac, A.; Rouessac, F. *Tetrahedron* **1978**, *34*, 19. (e) Sauer, J.; Sutsmann, R. *Angew. Chem., Int. Ed. Engl.* **1980**, *19*, 779. (f) Sauer, J. *Angew. Chem., Int. Ed. Engl.* **1967**, *6*, 16. (g) Sauer, J. *Angew. Chem., Int. Ed. Engl.* **1966**, *5*, 211. (h) Wasserman, A. *Diels-Alder Reactions*; Elsevier: New York, 1965.

(14) Dewar, M. J. S. *Angew. Chem., Int. Ed. Engl.* **1971**, *10*, 761. Dewar, M. J. S.; Jie, C. *Acc. Chem. Res.* **1992**, *25*, 537. Fukui, K. *Acc. Chem. Res.* **1971**, *4*, 57. Herndon, W. C. *Chem. Rev.* **1972**, *72*, 157. Houk, K. N. *Acc. Chem. Res.* **1975**, *8*, 361. Houk, K. N.; Li, Y.; Evanseck, J. D. *Angew. Chem., Int. Ed. Engl.* **1992**, *31*, 682. Sustmann, R. *Pure Appl. Chem.* **1974**, *40*, 569.

(15) Dewar, M. J. S. *J. Am. Chem. Soc.* **1984**, *106*, 209.

0022-3263/95/1960-6717$09.00/0

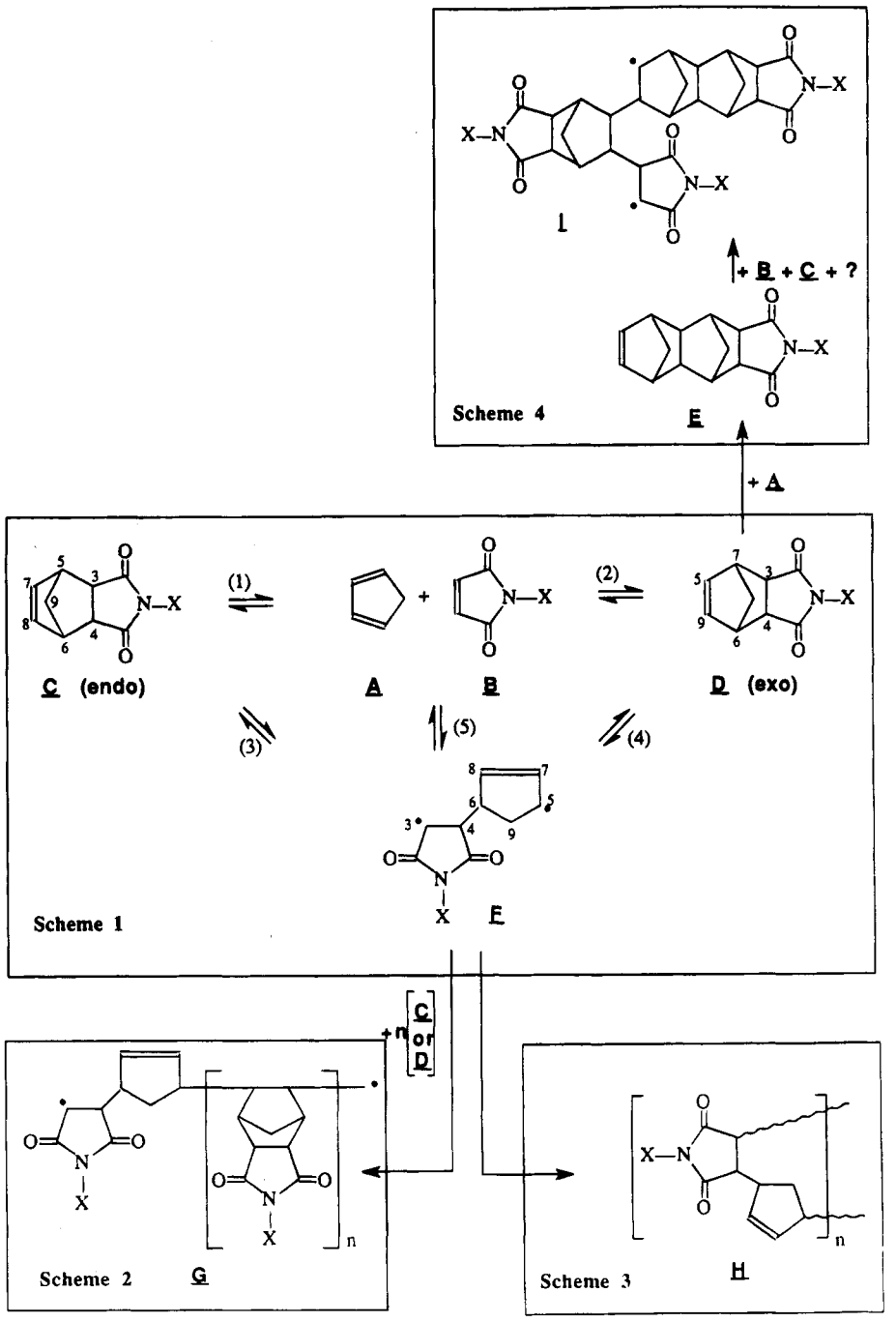

Figure 1. Possible isomerization and polymerization mechanisms in nadimide end-capped PMR prepolymers.

The currently assumed mechanisms of isomerization are represented in Scheme 1 of Figure 1. Depending on the nature of the diene and the dienophile, isomerization may be viewed as the following:

(i) Either an "external" process driven by a retro Diels–Alder reaction followed by a recombination of the addends to give the exo compound[9,10a,16] (steps 1 and 2 in Scheme 1 of Figure 1). Identification of cyclopentadiene **A** in the volatile products supported this mechanism.[2c,3a,b,5] In the same way, the formation of the doubly bridged adducts **E**, which can be interpreted as the result of the reaction of cyclopentadiene with *exo*-nadimide **D** acting as a dienophile, seems to confirm the contribution of a retro Diels–Alder reaction to the mechanism of isomerization.[2c,3a,b,17]

(ii) Or an "internal" route without dissociation into kinetically free fragments.[10] This process (steps 3 and 4 in Scheme 1 of Figure 1) starts with the cleavage of one of the Diels–Alder C–C bonds, e.g. C_3–C_5 in the endo adduct (step 3), followed by only one direct or several successive intramolecular hydrogen atom transfers from position C_9 to C_8 and finally recyclization between C_3 and C_7 giving the exo isomer. Thus, step 4 is a multistep process involving a biradical species of type **E**. Several experimental studies dealing with Diels–Alder reactions of N-substituted nadimides[3,8] concurred showing the production, together with N-substituted maleimide **B**, of significant quantities of N-substituted succinimides. These results, which have been interpreted in terms of hydrogen atom transfer, support a possible contribution

(16) Fox, M. A.; Cardona, R.; Kiwiet, N. J. *J. Org. Chem.* **1987**, *52*, 1469.

(17) Grenier-Loustalot, M. F.; Grenier, P. *High Perf. Polym.* **1991**, *3*, 263.

of such processes to the internal pathway. Finally, step 5 probably interconnects external and internal routes through the biradical intermediate **F**.

In addition to the isomerization scheme, three of the most frequently postulated polymerization schemes are displayed in Figure 1. Two of them (Schemes 2 and 3) require the contribution of the biradical species **F** previously involved in the isomerization pathway:

(i) In Scheme 2 the biradical initiates the homopolymerization of the norbornene rings thus leading to a polymer with a **G** type structure.[2c,3b,6]

(ii) In Scheme 3 the same intermediate yields an unsaturated alternating polymer of type **H**.[3b,5b,7] Such a structure within the polymer is consistent with the presence of an IR absorption at 743 cm^{-1} attributable to the cyclopentene crosslink.[18]

The last polymerization process, depicted in Scheme 4, does not necessarily involve the biradical species **F**. From *endo*-nadimide **C** and via *exo*-nadimide **D** a material like **I** is obtained which is almost devoid of olefinic functional group.[3b,19]

The present paper provides a semiempirical approach to the thermal properties of polyimides. To model the reactive end-caps of these systems we turned to the simplest substrate with a preformed imide moiety, e.g. nadimide. We shall focus only on the mechanism of isomerization (Scheme 1, Figure 1) with a special attention for **F**-type intermediates which have been designated in literature as the keystone species involved in some thermal curing processes.

A vast amount of theoretical work has been expanded on Diels–Alder reactions. To the best of our knowledge only a few authors have considered the stepwise mechanism as an alternative to the classical concerted mechanism.[15,20] In a semiempirical study by Dewar et al.[20a] step 1 or 2 is described within the closed-shell formalism, and steps 3 and 5 are described within the open-shell formalism, thus making critical any comparison between the different mechanisms. In the present work a single formalism will be used for the description of the entire isomerization potential energy surface.

In section I the first test of the reliability of our approach is to reexamine the textbook example of butadiene–ethylene. Next, the perturbation caused by a carbonyl group on reaction rates, stereochemistry, and regioselectivity will be scrutinized. In this respect, our computational effort will be directed at the cyclopentadiene–ethylene and cyclopentadiene–acrolein systems for which the results will be compared to experiment and ab initio values where available. Section II deals with the timing of the C–C bond breaking (step 1 or steps 3+5) and reforming (step 2) processes in the endo/exo isomerization of nadimide. The question of a possible contribution to the multistep process 4 of an intramolecular hydrogen atom transfer involving succinimide or biradical intermediates will be investigated. Finally, the origins of the sensitivity of rates to changes in the nature of the reaction medium have been sought in solvation and internal pressure effects.

Computational Details

The AM1 approximation to molecular orbital theory[21] as implemented in the AMPAC computer program[22] was used throughout this study. This method has been previously shown to provide accurate results for Diels–Alder reactions[16,20a–d,23,24] and intramolecular hydrogen transfer reactions.[23e,25,26]

As far as we are especially concerned with the conversion of a closed-shell system of reactants to an open-shell intermediate, probably a biradical species, via a transition state lying somewhere in between, an approach to the problem questioned in this work may be through an open-shell SCF treatment (half electron type calculation, HE[20a,27]) followed by a limited configuration interaction.

It is well known that the bonding changes in the Diels–Alder reaction between butadiene and ethylene can be qualitatively confined to the four electrons and four MO's of the diene and the two electrons and two MO's of the dienophile.[20e,l] Thus, such a system can be adequately described within the framework of a 6-in-6 complete active space (CAS).

Extension of the π system on the diene or the dienophile requires a priori that the active MO's space must be enlarged. Because of dimensional constraint inherent in the program the corresponding CAS CI will be truncated beyond 400 configurations and the continuity of the potential energy surface will not be preserved.

(18) Aso, C.; Kunitake, T.; Ishimoto, Y. *J. Polym. Sci.* **1968**, (A-1), *6*, 1163.

(19) Experimental evidence for the quasiabsence of insaturation has been provided by solid state NMR data (Grenier-Loustalot, M. F., unpublished results).

(20) (a) Dewar, M. J. S.; Olivella, S.; Stewart, J. J. P. *J. Am. Chem. Soc.* **1986**, *108*, 5771. (b) Branchadell, V.; Oliva, A.; Bertrán, J. *J. Mol. Struct.* **1985**, *120*, 85. (c) Moyano, A.; Olivella, S. *J. Mol. Struct. (Theochem)* **1990**, *208*, 261. (d) Kaila, N.; Franck, R. W.; Dannenberg, J. J. *J. Org. Chem.* **1989**, *54*, 4206. (e) Bernardi, F.; Bottoni, A.; Field, M. J.; Guest, M. F.; Hillier, I. H.; Robb, M. A.; Venturini, A. *J. Am. Chem. Soc.* **1988**, *110*, 3050. (f) Ortega, M.; Oliva, A.; Lluch, J. M.; Bertrán, J. *Chem. Phys. Lett.* **1983**, *102*, 317. (g) Townshend, R. E.; Ramunni, G.; Segal, G.; Hehre, W. J.; Salem, L. *J. Am. Chem. Soc.* **1976**, *98*, 2190. (h) Oliva, A.; Fernandez-Alonso, J. I.; Bertrán, J. *An. Quim.* **1979**, *75*, 45. (i) Dewar, M. J. S.; Chantranupong, L. *J. Am. Chem. Soc.* **1983**, *105*, 7152. (j) Dewar, M. J. S.; Pierini, A. B. *J. Am. Chem. Soc.* **1984**, *106*, 203. (k) Basilevsky, M. V.; Shamov, A. G.; Tikhomirov, V. A. *J. Am. Chem. Soc.* **1977**, *99*, 1369. (l) Li, Y.; Houk, K. N. *J. Am. Chem. Soc.* **1993**, *115*, 7478. (m) Dewar, M. J. S.; Olivella, S.; Rzepa, H. S. *J. Am. Chem. Soc.* **1978**, *100*, 5650. (n) Dewar, M. J. S.; Griffin, A. C.; Kirschner, S. *J. Am. Chem. Soc.* **1974**, *96*, 6225. (o) Bach, R. D.; MacDouall, J. J. W.; Schlegel, H. B.; Wolber, G. J. *J. Org. Chem.* **1989**, *54*, 2931.

(21) Dewar, M. J. S.; Zoebisch, E. G.; Healy, E. F.; Stewart, J. J. P. *J. Am. Chem. Soc.* **1985**, *107*, 3902.

(22) Dewar, M. J. S.; Stewart, J. J. P. Program No. 506. *QCPE Bull.* **1988**, *6*, 24.

(23) (a) Branchadell, V.; Font, J.; Oliva, A.; Orti, J.; Ortuño, R. M.; Rafel, S.; Terris, N.; Ventura, M. *Tetrahedron* **1991**, *47*, 8775. (b) Cativiela, C.; Garcia, J. I.; Mayoral, J. A.; Royo, A. J.; Salvatella, L. *J. Phys. Org. Chem.* **1992**, *5*, 230. (c) Houk, K. N.; Loncharich, R. J.; Blake, J. F.; Jorgensen, W. L. *J. Am. Chem. Soc.* **1989**, *111*, 9172. (d) Sodupe, M.; Oliva, A.; Bertrán, J.; Dannenberg, J. J. *J. Org. Chem.* **1989**, *54*, 2488. (e) Dannenberg, J. J. *Advances in Molecular Modeling*; Liotta, D., Ed.; JAI Press: Greenwich, CT, 1990; Vol. 2, p 1. (f) Lehd, M.; Jensen, F. *J. Org. Chem.* **1990**, *55*, 1034. (g) Jursic, B. S.; Zdravkovski, Z. *J. Mol. Struct. (Theochem)* **1994**, *309*, 249. (h) Thietze, L. F.; Fennen, J.; Anders, E. *Angew Chem.* **1989**, *101*, 1420.

(24) Dols, P. P. M. A.; Klunder, A. J. H.; Zwanenburg, B. *Tetrahedron Lett.* **1993**, *34*, 3181. Kraus, G. A.; Li, J.; Gordon, M. S.; Jensen, J. H. *J. Am. Chem. Soc.* **1993**, *115*, 5859. Werstiuk, N. H.; Jiangong, M.; Macaulay, J. B.; Fallis, A. G. *Can. J. Chem.* **1992**, *70*, 2798. Coll, G.; Costa, A.; Deya, P. M.; Flexas, F.; Rotger, C.; Saa, J. M. *J. Org. Chem.* **1992**, *57*, 6222. Wiest, O.; Steckhan, E.; Grein, F. *J. Org. Chem.* **1992**, *57*, 4034. Coxon, J. M.; Mac Donald, D. Q. *Tetrahedron Lett.* **1992**, *33*, 651. Boger, D. L.; Corbett, W. L.; Curran, T. T.; Kasper, A. M. *J. Am. Chem. Soc.* **1991**, *113*, 1713. Guner, O. F.; Lammertsma, K.; Alston, P. V.; Ottenbrite, R. M.; Shillady, D. D. *J. Org. Chem.* **1990**, *55*, 28. Barluenga, J.; Sordo, T. L.; Sordo, J. A.; Fustero, S.; Gonzalez, J. *J. Mol. Struct. (Theochem)* **1994**, *315*, 63.

(25) (a) Huang, X. L.; Dannenberg, J. J. *J. Org. Chem.* **1991**, *56*, 5421. (b) Lluch, J. M.; Bertrán, J.; Dannenberg, J. J. *Tetrahedron* **1988**, *24*, 7621.

(26) Trigueros, P. P.; Casanovas, J.; Aleman, C.; Vega, M. C. *J. Mol. Struct. (Theochem)* **1992**, *277*, 117.

(27) Dewar, M. J. S.; Hashmall, J. A.; Venier, C. G. *J. Am. Chem. Soc.* **1968**, *40*, 1953.

Table 1. Diels–Alder Reaction between *cis*-1,3-Butadiene and Ethylene: AM1-HE-SDCI Calculated Heats of Formation, Activation Enthalpies, and Key Structural Features of the Critical Points Located on the Potential Energy Surface

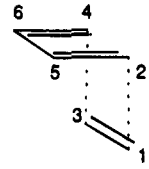

critical points	index	r_1 (Å)[a]	r_2 (Å)[a]	ω (deg)[b]	$\Delta_f H°$ (kJ mol^{-1})	activation enthalpies from reactants (kJ mol^{-1})	activation enthalpies from products (kJ mol^{-1})
butadiene + ethylene	0	6.000	6.000		100.7	0	
TS_c	1	2.115	2.115	50.7	216.1	115.4	288.0
TS_{as}	1	1.870	4.027	110.4	233.8	133.1	305.7
M_{as}	0	1.523	4.227	91.0	175.0		
TS_d	1	1.525	2.902	74.6	176.1		248.0
cyclohexene	0	1.518	1.518	44.2	−71.9		0

[a] $r_1 = 1-2$; $r_2 = 3-4$. [b] ω: Dihedral angle 5-2-1-3.

In the present work, in order to take into account these constraints at best, the active MO's space will be extended to the four HOMO's and the four LUMO's and configuration interaction will be performed by using the complete SDCI space (thus including only mono and diexcited configurations, i.e. 361 configurations).

Full optimization of the geometries in an internal coordinates frame was performed with the keywords PRECISE and PULAY. Minima were found using the standard Davidon–Fletcher–Powell minimization scheme[28] or the Powell method.[29]

Transition states were located with the aid of the algorithm CHAIN.[30] By shifting along the gradient vector field of an arbitrary continuous path linking reactants and products, a limiting path is obtained, the highest point of which is a saddle point. At the end of this procedure, relaxation of the geometry of the saddle points provides the different connections between reactants, products, and stable intermediates. The number λ of the negative eigenvalues of the matrix of second derivatives required to characterize the stationnary points as minima ($\lambda = 0$), transition states ($\lambda = 1$) or critical points with index $\lambda \geq 2$ was calculated for each optimized structure. Accuracy on the eigenvalues of the matrix of second derivatives was estimated to be better than 5%.

I. *cis*-1,3-Butadiene + Ethylene, Cyclopentadiene + Ethylene, and Cyclopentadiene + Acrolein as Tests for the Open-Shell AM1-HE-SDCI Procedure. (1) *cis*-1,3-Butadiene + Ethylene System. We will start an evaluation of the previously described procedure with the prototype Diels–Alder reaction between *cis*-1,3-butadiene and ethylene which has been extensively investigated by ab initio[20e-g,l,o,23c,31] and semiempirical calculations.[15,20a,h-k,m,n,23e-h,32]

Our results are summarized in Table 1. The first measure of the accuracy of the procedure for the butadiene–ethylene system may be through the reproduction of the heat of reaction. The reaction of butadiene plus ethylene to form cyclohexene is calculated to be exothermic by 172.6 kJ mol^{-1}, in good agreement with the experimental value of 161.1 kJ mol^{-1}.[33] Our AM1 model fairly concurs with ab initio results (cf. the 158.8 kJ mol^{-1} RHF/3-21G value of Li and Houk[20l]).

A transition state of C_S symmetry (TS_c) has been located, involving the synchronous formation (or scission) of the two Diels–Alder C–C bonds. The activation enthalpy $\Delta_r H°^{\ddagger}$ on the input concerted channel is calculated to be 115.4 kJ mol^{-1}, a value which falls in the range of the most recent high level ab initio results of Houk et al. (106.6–122.9 kJ mol^{-1} [20l,31c]). In addition, our $\Delta_r H°^{\ddagger}$ value is higher than the semiempirical closed-shell estimates obtained without configuration interaction (AM1: 99.5 kJ mol^{-1} [20a,23f] and 99.1 kJ mol^{-1} [23g] and PM3: 113.3 kJ mol^{-1} [23g]).

In the asynchronous zone of the potential energy surface only one transition state of diradicaloid nature (TS_{as}) was localized with the methylene radical center rotated somewhere between syn gauche and trans to the allyl moiety. This result is in agreement with CASSCF/3-21G and CASSCF/6-31G* calculations by Houk et al.[20l,31c] The calculated activation enthalpy for the one Diels–Alder C–C bond formation is found to be 133.1 kJ mol^{-1}.

From TS_{as}, a diradical intermediate M_{as} is attained which has been identified as a true minimum on the basis of the eigenvalues of the hessian. As expected, the final step of the reaction, leading to cyclohexene, proceeds via TS_d without almost any barrier ($\Delta_r H°^{\ddagger} = 1.1$ kJ mol^{-1}).

With respect to the reaction of formation of cyclohexene it appears that the one-bond addition scheme is less favorable by 17.7 kJ mol^{-1} than the concerted route. This theoretical value is in line with both the CASSCF/3-21G estimate of Li et al. (14.2 kJ mol^{-1} [20l]) and the experimental "energy of concert" (8–29 kJ mol^{-1} [34]) as defined by Doering.[34a]

Rate constant measurement at 800 K for the reaction of butadiene and ethylene led to an activation energy of 114.9 kJ mol^{-1}.[35] Assuming that the activation enthalpy $\Delta_r H°^{\ddagger}$ is independant of the temperature, the activation

(28) Davidon, W. C. *Comput. J.* **1968**, *10*, 406. Fletcher, R.; Powell, M. J. D. *Comput. J.* **1963**, *6*, 163.

(29) Powell, M. J. D. *Numerical Methods for Linear Algebraic Equations*; Rabinowitz, Ed.; Gordon & Breach: New York, 1970; Chap. 6 and 7.

(30) Liotard, D. *Symmetries and properties of non rigid molecules*; Maruani, J., Serre, J., Eds.; Elsevier: New York, 1983.

(31) (a) Brown, F. K.; Houk, K. N. *Tetrahedron Lett.* **1984**, *25*, 4609. (b) Houk, K. N.; Lin, Y. T.; Brown, F. K. *J. Am. Chem. Soc.* **1986**, *108*, 554. (c) Houk, K. N.; Li, Y.; Storer, J.; Raimondi, L.; Beno, B. *J. Chem. Soc., Faraday Trans.* **1994**, *90*, 1599. (d) Burke, L. A.; Leroy, G.; Sana, M. *Theor. Chim. Acta* **1975**, *40*, 313. (e) Burke, L. A.; Leroy, G. *Theor. Chim. Acta* **1977**, *44*, 219. (f) Craig, S. L.; Stone, A. J. *J. Chem. Soc., Faraday Trans.* **1994**, *90*, 1663.

(32) (a) Caramella, P.; Houk, K. N.; Domelsmith, L. *J. Am. Chem. Soc.* **1977**, *99*, 4511. (b) Herndon, W.; Hall, L. *Tetrahedron Lett.* **1967**, *32*, 3095. (c) Jug, K.; Kruger, H. W. *Theor. Chim. Acta* **1979**, *52*, 19. (d) Kikuchi, O. *Tetrahedron* **1971**, *27*, 2791. (e) MacIver, J. W., Jr. *Acc. Chem. Res.* **1974**, *7*, 72.

(33) Rossini, F. D.; Pitzer, K. S.; Arnett, R. L.; Braun, R. M.; Pimentel, G. C. *Selected values of physical and thermodynamic properties of hydrocarbons and related compounds*; Carnegie Press: Pittsburg 1953.

Table 2. Diels–Alder Reaction between Cyclopentadiene and Ethylene: AM1-HE-SDCI Calculated Heats of Formation, Activation Enthalpies, and Key Structural Features of the Critical Points Located on the Potential Energy Surface

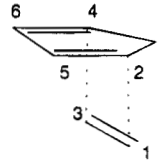

critical points	index	r_1 (Å)[a]	r_2 (Å)[a]	ω (deg)[b]	$\Delta_f H°$ (kJ mol^{-1})	activation enthalpies from reactants (kJ mol^{-1})	activation enthalpies from products (kJ mol^{-1})
cyclopentadiene + ethylene	0	6.000	6.000		136.3	0	
TS_c[c]	1	2.094	2.094		262.0	125.7	183.0
TS_t	1	1.877	4.323	−173.5	257.9	121.6	178.9
M_t	0	1.518	4.451	−175.3	198.9		
TS_{sg}	1	1.875	3.411	70.0	264.7	128.4	185.7
M_{sg}	0	1.513	3.781	60.8	204.5		
TS_{ag}	1	1.880	4.667	−75.4	260.1	123.8	181.1
M_{ag}	0	1.516	4.769	−72.2	200.0		
R1	1	1.524	3.923	120.1	214.1		
R2	1	1.520	4.815	−124.5	205.0		
R3	1	1.515	4.205	−5.3	213.5		
TS_d	1	1.540	2.675	67.2	225.1		146.1
norbornene	0	1.548	1.548	67.3	79.0		0

[a] $r_1 = 1-2$; $r_2 = 3-4$. [b] ω: Dihedral angle 5-2-1-3. [c] AM1-RHF-SDCI calculation.

energy E_a may be expressed as follows:

$$E_a = \Delta_r H°^{\ddagger} + nRT \quad (1)$$

where n represents the molecularity of the process.

Thus, the experimental activation enthalpy to be compared with our theoretical estimate (115.4 kJ mol^{-1}) is 101.6 kJ mol^{-1}. The other AM1 values of ca. 99 kJ mol^{-1} obtained without configuration interaction are in this case better than our result.

For the reaction of decyclization of cyclohexene, the one Diels–Alder C–C bond cleavage is easier by 40 kJ mol^{-1} than the simultaneous rupture of the two Diels–Alder C–C bonds. Insofar as the scission of the second C–C bond requires an additional amount of energy of ca. 57.7 kJ mol^{-1} (a quantity corresponding to the energy gap between TS_d and TS_{as}) the reverse process appears as preferentially synchronous. Therefore, the most accessible pathway for the retro Diels–Alder reaction involves an activation enthalpy of 288 kJ mol^{-1}.

The gas phase pyrolytic decyclization of cyclohexene has been studied experimentally.[36] A concerted mechanism has been postulated. Using the most recent experimental value of the activation energy E_a as 272 ± 12 kJ mol^{-1} at 773 K[36] the reaction would have an activation enthalpy $\Delta_r H°^{\ddagger}$ ranging from 254 to 278 kJ mol^{-1}. Here, our theoretical estimate for the synchronous process (288 kJ mol^{-1}) is clearly in better accordance with experimental data than the AM1 closed-shell value of Lehd et al. (335.2 kJ mol^{-1} [23f]) obtained without configuration interaction.

In this section we have just checked the ability of an open-shell AM1-SDCI procedure to mimic ab initio results and to reproduce experimental data for the well documented butadiene–ethylene system. On the basis of these preliminary tests, the first conclusion to be drawn is that an open-shell formalism can handle both the synchronous concerted and stepwise processes in Diels–Alder reactions without always leading to the so claimed "unnatural" preference for a diradical mechanism.

In the following, we will try to gauge its predictive capacity to reproduce substituent effects on mechanistic features and rates of Diels–Alder reactions. Placing a carbonyl group on ethylene would be expected to enhance its dienophilicity. Therefore, a detailed comparative analysis of the reaction mechanisms for the cyclopentadiene–ethylene and cyclopentadiene–acrolein systems will be presented.

(2) Cyclopentadiene + Ethylene System. Energetics and key structural features of the critical points of chemical interest, i.e. reactants, transition states, and products, are displayed in Table 2.

Within the framework of the above AM1-HE-SDCI treatment, the TS_c transition state on the concerted addition pathway appears as slightly nonsymmetrical with the two Diels–Alder C–C bonds at 2.002 and 2.220 Å. Such a dissymmetry has never been reported in literature[23c,g,37] so that the question is whether this result is an artefact of our procedure or not. First of all, we have verified that the dissymmetry remains when the active space selected in the calculation includes only the six classical MO's[20e,l] (the two forming C–C bond lengths are calculated to be 2.006 and 2.212 Å). Actually, we have found that, in an open-shell SCF treatment (HE procedure), a permutation between the highest doubly occupied MO and the lowest singly occupied MO during the search of the transition state is probably the cause of the dissymmetry. By using a closed-shell MO's set (RHF procedure) and starting from the nonsymmetrical transition state we obtain finally a symmetrical transition state with the two Diels–Alder C–C bonds at 2.094 Å (Table 2).

With regard to energetical considerations the concerted process requires an activation enthalpy of 125.7 kJ mol^{-1}, comparable to other theoretical estimates (AM1: 117.0 kJ mol^{-1},[23g] PM3: 134.2 kJ mol^{-1},[23g] RHF/3-21G: 125.8 kJ mol^{-1} [37]).

(34) (a) Doering, W. V. E.; Roth, W. R.; Breuckmann, R.; Fige, L.; Lennartz, H. W.; Fessner, W. D.; Prinsbach, H. *Chem. Ber.* **1988**, *121*, 1. (b) Frey, H. M.; Pottinger, R. J. *J. Chem. Soc., Faraday Trans. 1* **1977**, *74*, 1827.

(35) Rowley, D.; Steiner, H. *Diss. Faraday Soc.* **1951**, *10*, 198.

(36) Tardy, D. C.; Ireton, R.; Gordon, A. S. *J. Am. Chem. Soc.* **1979**, *101*, 1508.

(37) Jorgensen, W. L.; Lim, D.; Blake, J. F. *J. Am. Chem. Soc.* **1993**, *115*, 2936.

Table 3. Diels–Alder Reaction between Cyclopentadiene and *cis*-Acrolein: AM1-HE-SDCI Calculated Heats of Formation, Activation Enthalpies, and Key Structural Features of the Critical Points Located on the Potential Energy Surface

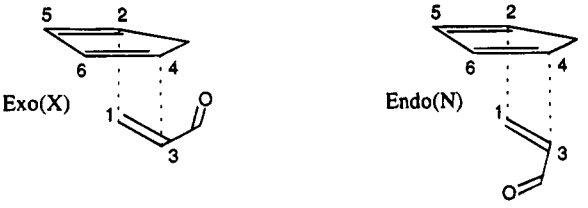

critical points	index	r_1 (Å)[a]	r_2 (Å)[a]	ω (deg)[b]	$\Delta_f H°$ (kJ mol^{-1})	activation enthalpies from reactants (kJ mol^{-1}) endo	exo	activation enthalpies from products (kJ mol^{-1}) endo	exo
reactants	0	6.000	6.000		3.6		0		
(N) TS_c	1	1.932	2.417	−71.4	130.6	127.0		153.7	
(X) TS_c	1	1.940	2.397	−64.8	125.1		121.5		164.8
(N) TS_t (1,2)	1	1.864	4.406	168.0	114.8	111.2		137.9	
(X) TS_t (1,2)	1	1.863	4.288	177.3	115.7		112.1		155.4
(N) TS_{sg} (1,2)	1	1.863	3.423	−70.9	124.3	120.7		147.4	
(X) TS_{sg} (1,2)	1	1.863	3.456	−63.1	120.4		116.8		160.1
(N) TS_{ag} (1,2)	1	1.864	4.630	69.4	118.2	114.6		141.3	
(X) TS_{ag} (1,2)	1	1.864	4.677	77.9	119.9		116.3		159.6
(N) TS_d (1,2)	1	1.543	2.690	−71.3	91.9			115.0	
(X) TS_d (1,2)	1	1.544	2.701	−64.3	87.1				126.8
(N) TS_t (3,4)	1	4.389	1.878	−177.1	143.4	139.8		166.5	
(X) TS_t (3,4)	1	4.318	1.870	−175.3	139.2		135.6		178.9
(N) TS_{sg} (3,4)	1	3.459	1.869	61.8	148.3	144.7		171.4	
(X) TS_{sg} (3,4)	1	3.377	1.869	68.6	143.8		140.2		183.5
(N) TS_{ag} (3,4)	1	4.611	1.872	−63.0	142.7	139.1		165.8	
(X) TS_{ag} (3,4)	1	4.767	1.883	−80.7	147.7		144.1		187.4
(N) TS_d (3,4)	1	2.687	1.547	68.3	114.6			137.7	
(X) TS_d (3,4)	1	2.667	1.550	67.8	115.8				155.5
(N) adduct	0	1.549	1.555	−69.0	−23.1			0	
(X) adduct	0	1.548	1.556	−66.6	−39.7			0	

[a] r_1 = 1–2; r_2 = 3–4. [b] Dihedral angle ω: 5-2-1-3 for adducts, TS_c and (1,2) transition states, 6-4-3-1 for (3,4) transition states.

The one-bond asynchronous addition can proceed via three possible unsymmetrical transition states. These critical points (TS_t, TS_{ag}, TS_{sg}) differ essentially from each other by the value of the dihedral angle ω describing the relative position of the cyclopentadiene and ethylene fragments around the forming bond. Two of them lie slightly lower than the TS_c transition state by, respectively, 4.1 kJ mol^{-1} (TS_t) and 1.9 kJ mol^{-1} (TS_{ag}). The third one, TS_{sg}, is less stable than TS_c by 2.7 kJ mol^{-1}. Three nearly energetically equivalent structures (M_t, M_{ag}, M_{sg}) of biradical nature were also located that could serve as intermediates for the nonsynchronous processes. These minima are connected by a rotational mode ω. Along this mode, three critical points, R_1, R_2, R_3 with ω values, respectively, intermediate between values for M_t and M_{sg}, M_t and M_{ag}, and M_{sg} and M_{ag} were identified as conformational transition states. The ring closure from M_{sg} to norbornene passes through TS_d with a low activation enthalpy ($\Delta_r H°^{\ddagger}$ = 20.6 kJ mol^{-1}). As previous authors have confined their study to the synchronous region of the potential energy surface,[23c,g,37] no other theoretical data are available for comparison with these predictions.

The small differences between the four entrance barriers suggest that both the concerted and stepwise mechanisms can model the addition of ethylene on cyclopentadiene. Together with those produced by AM1,[23g] PM3,[23g] and ab initio RHF/3-21G calculations[23c] our activation enthalpies are substantially higher than the experimental value (98.9 ± 6 kJ mol^{-1} [38]).

It must be mentioned that, only from ab initio calculations including electron correlation evaluated at MP3 level, a closer fit to experimental data has been obtained ($\Delta_r H°^{\ddagger}$ = 90.5 kJ mol^{-1} computed at the MP3/6-31G*//6-31G* level by Jorgensen et al.[37]).

For the decyclization of norbornene the rate-determining step is associated to TS_t but TS_c, TS_{sg}, and TS_{ag} are nearly equally competitive. The four calculated barriers lie within the experimental 178.7–186.2 kJ mol^{-1} range.[38,39] Consistency with experiment is here clearly superior to that observed for the forward reaction.

(3) Cyclopentadiene–Acrolein System. With the purpose of modeling the effect of unsymmetrical substitution of the dienophile by a formyl group on the course of Diels–Alder reactions we provide in the present section a detailed picture of the potential energy surface of the cyclopentadiene–acrolein system.

In both endo (N) and exo (X) approaches acrolein can adopt either the cis or the trans conformation. Energetics and key structural features of the critical points of chemical interest, i.e. reactants, transition states and products are displayed in Table 3 (cis formyl group) and Table 4 (trans formyl group). In the rotational space of the biradical region of the surface 24 additional minima of M_t, M_{ag}, or M_{sg} type were located. Their geometrical and energetical characteristics are available on request in the form of supporting information.

The formyl substituent makes the concerted transition state structures (TS_c) highly unsymmetrical with forming

(38) Walsh, R.; Wells, J. M. *J. Chem. Soc., Perkin Trans. 2* **1976**, 52.

(39) (a) Herndon, W. C.; Cooper, W. B., Jr.; Chambers, M. J. *J. Chem. Phys.* **1964**, *68*, 2016. (b) Roquitte, B. C. *J. Phys. Chem.* **1965**, *69*, 1351.

Table 4. Diels–Alder Reaction between Cyclopentadiene and *trans*-Acrolein: AM1-HE-SDCI Calculated Heats of Formation, Activation Enthalpies, and Key Structural Features of the Critical Points Located on the Potential Energy Surface

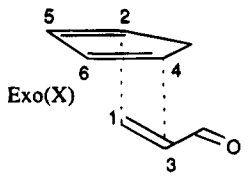

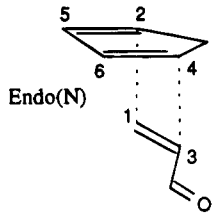

critical points	index	r_1 (Å)[a]	r_2 (Å)[a]	ω (deg)[b]	$\Delta_f H°$ (kJ mol^{-1})	activation enthalpies from reactants (kJ mol^{-1}) endo	exo	activation enthalpies from products (kJ mol^{-1}) endo	exo
reactants	0	6.000	6.000		2.1		0		
(N) TS_c	1	1.946	2.368	−72.4	126.2	124.1		150.5	
(X) TS_c	1	1.955	2.352	−65.0	126.4		124.3		166.4
(N) TS_t (1,2)	1	1.872	4.374	171.4	117.2	115.1		141.5	
(X) TS_t (1,2)	1	1.871	4.298	175.9	116.2		114.1		156.2
(N) TS_{sg} (1,2)	1	1.869	3.408	−73.6	122.7	120.6		147.0	
(X) TS_{sg} (1,2)	1	1.869	3.412	−68.2	123.5		121.4		163.5
(N) TS_{ag} (1,2)	1	1.872	4.622	69.9	118.8	116.7		143.1	
(X) TS_{ag} (1,2)	1	1.874	4.664	74.6	118.4		116.3		158.4
(N) TS_d (1,2)	1	1.543	2.706	−70.6	88.8			113.1	
(X) TS_d (1,2)	1	1.543	2.688	−64.3	87.9				127.9
(N) TS_t (3,4)	1	4.313	1.879	178.1	143.6	141.5		167.9	
(X) TS_t (3,4)	1	4.280	1.874	−179.6	138.3		136.2		178.3
(N) TS_{sg} (3,4)	1	3.400	1.866	66.0	140.9	138.8		165.2	
(X) TS_{sg} (3,4)	1	3.398	1.870	72.0	140.3		138.2		180.3
(N) TS_{ag} (3,4)	1	4.603	1.876	−61.7	137.5	135.4		161.8	
(X) TS_{ag} (3,4)	1	4.720	1.879	−70.6	140.6		138.5		180.6
(N) TS_d (3,4)	1	2.676	1.550	65.9	109.4			133.7	
(X) TS_d (3,4)	1	2.665	1.550	69.1	110.1				150.1
(N) adduct	0	1.551	1.558	−69.1	−24.3			0	
(X) adduct	0	1.549	1.556	−66.0	−40.0			0	

[a] r_1 = 1–2; r_2 = 3–4. [b] Dihedral angle ω: 5-2-1-3 for adducts, TS_c and (1,2) transition states, 6-4-3-1 for (3,4) transition states.

bonds of ~1.93–1.95 and 2.35–2.40 Å. These structural features resemble those calculated at the 6-31G* level for the transition states of the methyl vinyl ketone + cyclopentadiene reaction.[37] In agreement with previous results on Diels–Alder reactions between cyclopentadiene and unsymmetrical dienophiles the more fully formed bond is at the nonsubstituted carbon of the dienophile.[23c,37] The lowest concerted transition state is exo with acrolein in the cis conformation. The corresponding activation enthalpy from the reactants is 121.5 kJ mol^{-1}.

For both endo and exo one-bond approaches, two possible pathways exist depending on which end of the dienophile the first C–C bond is formed. The greater reactivity of the carbon β to the formyl group is reflected by the large coefficients of this carbon in the acrolein LUMO. The routes involving the formation of the C_3–C_4 bond (Tables 3 and 4) are less readily accessible than the others by ca. 16.8–28.6 kJ mol^{-1}. Therefore, they are likely to be dismissed on energetical grounds.

AM1-HE-SDCI calculations place the most favorable one-bond transition state, (N) TS_t (1,2) with the formyl group in cis conformation, 111.2 kJ mol^{-1} above the reactants. From this point, the shortest reaction pathway leads to the (N) adduct via successively a minimum of (N) M_t type ($\Delta_f H°$ = 67.5 kJ mol^{-1}), a rotational transition state of R_1 type ($\Delta_f H°$ = 82.7 kJ mol^{-1}), another minimum of (N) M_{sg} type ($\Delta_f H°$ = 68.6 kJ mol^{-1}), and the final ring closure transition state (N) TS_d (1,2) ($\Delta_f H°$ = 91.9 kJ mol^{-1}). Accordingly, the first step is rate determining for the stepwise process.

The most economical concerted transition state being only 10.3 kJ mol^{-1} higher in energy than the lowest one-bond transition state, the concerted mechanism cannot be reasonably excluded.

The experimental activation energy for the reaction of addition in the gas phase has been measured as 63.5 kJ mol^{-1} [40] thus showing a decrease of 35.4 kJ mol^{-1} in the barrier relative to the cyclopentadiene–ethylene system.

The accelerating effect of the formyl group is partially reproduced by our calculated data. The barrier is reduced by ~10 kJ mol^{-1} as compared to the nonsubstituted cycloaddition. Note that even at ab initio level the effect of the formyl group is difficult to reproduce. By replacing ethylene with acrolein in the butadiene–ethylene system the decrease of the barrier is only 2 kJ mol^{-1} at the STO 3G level[41] and 22.6 kJ mol^{-1} at the 3-21G level.[41,42]

Finally, one of the most important points from Tables 3 and 4 that should be noted refers to the reaction of decyclization. In accordance with previous studies,[12] of the two bonds that can break, the more highly substituted do so first. As for the direct process (N) TS_t (1,2) is the rate-determining transition state. Like for the butadiene–ethylene and cyclopentadiene–ethylene systems, the AM1-HE-SDCI procedure accurately predicts the activation enthalpy for the decomposition of endo

(40) Kistiakowsky, G. B.; Lacher, J. R. *J. Am. Chem. Soc.* **1936**, *58*, 123.

(41) (a) Loncharich, R. J.; Brown, F. K.; Houk, K. N. *J. Org. Chem.* **1989**, *54*, 1129. (b) Birney, D. M.; Houk, K. N. *J. Am. Chem. Soc.* **1990**, *112*, 4127.

(42) Menendez, M. I.; Gonzalez, J.; Sordo, J. A.; Sordo, T. L. *J. Mol. Struct. (Theochem)* **1994**, *314*, 241.

Table 5. Diels–Alder Reaction between Cyclopentadiene and Maleimide: Geometrical Parameters and Heats of Formation for Reactants and Adduct Products

geometrical parameters[a]	cyclopentadiene	maleimide	*endo*-nadimide	*exo*-nadimide
		Bond Lengths (Å)		
C_3-C_6, C_4-C_9			1.544	1.546
N_1-C_2, N_1-C_5		1.412	1.407	1.407
C_2-C_3, C_4-C_5		1.514	1.523	1.522
C_3-C_4		1.350	1.572	1.572
C_6-C_{10}, C_9-C_{10}	1.508		1.564	1.560
C_6-C_7, C_8-C_9	1.367		1.525	1.528
C_7-C_8	1.460		1.369	1.370
		Valence Angles (deg)		
$C_2-C_3-C_6, C_5-C_4-C_9$			115.0	113.5
$C_2-C_3-C_4, C_5-C_4-C_3$		108.4	104.7	104.6
$C_6-C_3-C_4, C_9-C_4-C_3$			103.4	103.3
$N_1-C_2-C_3, N_1-C_5-C_4$		106.8	108.9	109.2
$C_2-N_1-C_5$		109.6	112.8	112.4
$C_3-C_6-C_7, C_4-C_9-C_8$			106.5	104.2
$C_3-C_6-C_{10}, C_4-C_9-C_{10}$			99.8	101.4
$C_7-C_6-C_{10}, C_8-C_9-C_{10}$	109.3		99.7	99.6
$C_6-C_7-C_8, C_7-C_8-C_9$	109.2		107.5	107.4
$C_6-C_{10}-C_9$	102.9		94.0	94.2
heat of formation (kJ mol^{-1})		−8.6	−137.3	−163.3

[a] See Figure 2 for the definition of the atoms.

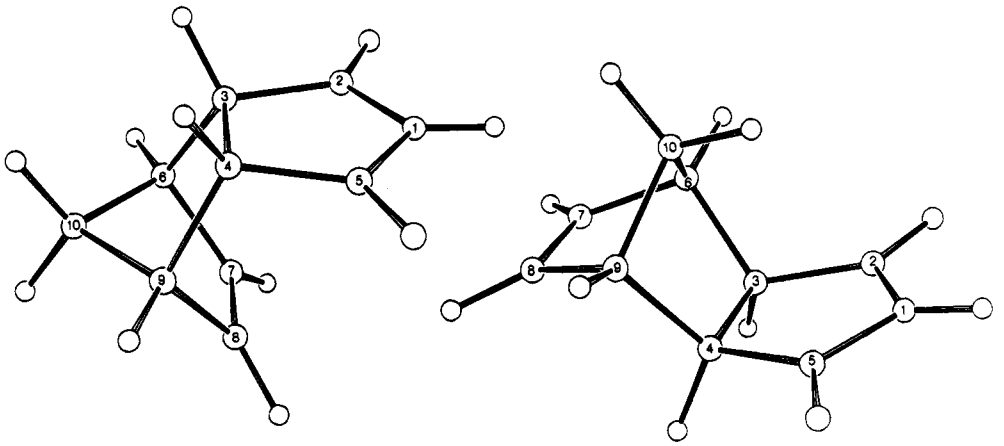

Figure 2. ORTEP plots of the AM1-HE-SDCI optimized geometries of the nadimide adducts.

methylene tetrahydrobenzaldehyde: 137.9 kJ mol^{-1} or 141.5 kJ mol^{-1} (depending on the conformation of the formyl group) versus 138 ± 5 kJ mol^{-1} as deduced from the experimental activation energy.[40] Therefore, our calculations give a very good account of the formyl substituent effect on the rate of the retro Diels–Alder reaction.

At this stage of the discussion some conclusions do emerge. Firstly, an AM1-HE-SDCI procedure is quite appropriate for the description of retro Diels–Alder reactions. A close fit to the experimental values of the barriers over a wide reactivity range (140–272 kJ mol^{-1}) has been obtained. The accelerating effect of the electron-withdrawing formyl group on the rate of decyclization has been accurately modeled. Therefore, the results of these preliminary tests seem the most encouraging for us in that they provide a basis for confidence in the computed barrier of the dissociative step of the epimerization of *endo*-nadimide.

With respect to the addition reactions the order of reactivity of the dienophiles is reasonably predicted but the barriers are grossly overestimated. As the barriers for the reverse processes are properly reproduced, a deficiency of the AM1-HE-SDCI procedure for the description of the reactants may be the cause of these differences. Besides, as claimed elsewhere,[41] it cannot be excluded that these discrepancies may originate from uncertainties in experimental data which may not be sufficiently accurate (shock tube experiments performed sometimes 50 years ago, presence of side reactions such as polymerization of the diene or rate measurements performed over a too narrow temperature range).

II. Cyclopentadiene–Maleimide System. (1) Geometrical Features and Relative Stabilities of Reactants and Products. AM1-HE-SDCI structural parameters of the skeleton and enthalpies of formation for cyclopentadiene, maleimide and the two corresponding adducts are given in Table 5. ORTEP plots for *endo*- and *exo*-nadimides are represented in Figure 2.

As expected, the adducts show a C_S symmetry. With regard to bond lengths they are quite similar: the C_3-C_4, C_6-C_7, and C_8-C_9 bonds have lengthened in comparison with those calculated in maleimide and cyclopentadiene, whereas, in accordance with a double bond character reinforcement, the C_7-C_8 bond is shorter than in cyclopentadiene. The two Diels–Alder bonds are equivalent to the other C–C single bonds. The other bond lengths are practically unaffected relative to those in cyclopentadiene and maleimide.

Table 6. Diels–Alder Endo Reaction between Cyclopentadiene and Maleimide: AM1-HE-SDCI Calculated Heats of Formation, Activation Enthalpies, and Key Structural Features of the Critical Points Located on the Potential Energy Surface

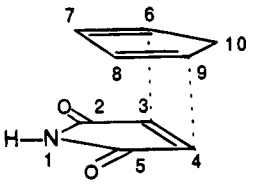

critical points	index	r_1 (Å)[a]	r_2 (Å)[a]	ω (deg)[b]	$\Delta_f H°$ (kJ mol^{-1})	activation enthalpies from reactants (kJ mol^{-1})	activation enthalpies from products (kJ mol^{-1})
cyclopentadiene + maleimide	0	6.000	6.000		−8.6	0	
TS_c	1	2.137	2.137	68.6	70.4	79.0	207.7
TS_t	1	1.950	4.220	52.1	76.9	85.5	214.2
M_t	0	1.517	4.496	67.2	−9.9		
TS_{sg}	1	1.953	3.373	−42.9	72.2	80.8	209.5
M_{sg}	0	1.514	3.847	−72.0	−15.2		
TS_{ag}	1	1.963	4.633	179.9	66.1	74.7	203.4
M_{ag}	0	1.520	4.704	180.2	−19.7		
R1	1	1.524	3.964	−6.4	−1.0		
R2	1	1.522	4.849	118.5	−4.4		
R3	1	1.517	4.317	−126.1	−12.1		
TS_d	1	1.541	2.701	−39.5	6.6		143.9
endo-nadimide	0	1.544	1.544	−36.4	−137.3		0

[a] r_1 = 4–9; r_2 = 3–6. [b] ω: Dihedral angle 3-4-9-10.

Table 7. Diels–Alder Exo Reaction between Cyclopentadiene and Maleimide: AM1-HE-SDCI Calculated Heats of Formation, Activation Enthalpies, and Key Structural Features of the Critical Points Located on the Potential Energy Surface

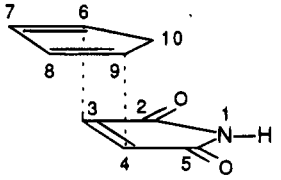

critical points	index	r_1 (Å)[a]	r_2 (Å)[a]	ω (deg)[b]	$\Delta_f H°$ (kJ mol^{-1})	activation enthalpies from reactants (kJ mol^{-1})	activation enthalpies from products (kJ mol^{-1})
cyclopentadiene + maleimide	0	6.000	6.000		−8.6	0	
TS_c	1	2.150	2.150		71.0	79.6	234.3
TS_t	1	1.959	4.272	69.6	65.6	74.2	228.9
M_t	0	1.519	4.383	61.4	−19.0		
TS_{sg}	1	1.960	3.494	−30.9	68.5	77.1	231.8
M_{sg}	0	1.517	3.738	−41.5	−17.2		
TS_{ag}	1	1.964	4.750	−180.1	77.4	86.0	240.7
M_{ag}	0	1.517	4.764	−180.8	−14.6		
R1	1	1.522	4.078	12.1	−8.7		
R2	1	1.522	4.839	123.0	−5.0		
R3	1	1.518	4.287	−122.3	0.5		
TS_d	1	1.539	2.668	−43.9	3.1		166.4
exo-nadimide	0	1.546	1.546	−35.3	−163.3		0

[a] r_1 = 4–9; r_2 = 3–6. [b] ω: Dihedral angle 3-4-9-10.

The absolute magnitude of the dihedral angle between the maleimide and the plane defined by the two Diels–Alder C–C bonds is slightly larger in the endo adduct (120.7°) than in the exo adduct (119.0°). The dihedral angle between the latter plane and the C_6–C_7–C_8–C_9 plane is decreased from 112.4° in the endo adduct to 109.8° in the exo adduct.

From the energetical point of view, the two Diels–Alder reactions are largely exothermic by 154.7 kJ mol^{-1} for the exo process and 128.7 kJ mol^{-1} for the endo process. The exo adduct appears to be more stable than the endo adduct by 26 kJ mol^{-1}, in agreement with the typical pattern of Diels–Alder reactions.[11,13,43]

(2) Main Features of the Potential Energy Surface. Tables 6 and 7 list the calculated heats of formation, activation enthalpies, and three basic geometrical parameters for the critical points located on the potential energy surface.

(a) Concerted Pathways. AM1-HE-SDCI calculated structural parameters of the concerted transition states (N) TS_c and (X) TS_c are listed in Table 8. The corresponding ORTEP plots are illustrated in Figure 3. The negative eigenvalue characterizing each structure is associated with a transition vector dominated by the C_3–C_6 and C_4–C_9 distances which describe the separation of the two fragments. These distances (~2.15 Å) are similar to those calculated for such concerted reactions.[16,20a,d–h,l,m,23a–g,31a–e,32a,37,41a,42]

The geometries of the cyclic moieties (Table 8) are only slightly affected relative to the reactants. The largest

(43) Tobis, D.; Harrison, R.; Phillips, B.; White, T. L.; Dimare, M.; Rickborn, B. *J. Org. Chem.* **1993**, *58*, 6701.

Table 8. Diels–Alder Reaction between Cyclopentadiene and Maleimide: Geometrical Parameters and Heats of Formation for the Synchronous Transition States

geometrical parameters[a]	(N) TS_c	(X) TS_c
Bond Lengths (Å)		
C_3-C_6, C_4-C_9	2.136	2.150
N_1-C_2, N_1-C_5	1.415	1.414
C_2-C_3, C_4-C_5	1.505	1.508
C_3-C_4	1.422	1.422
C_6-C_{10}, C_9-C_{10}	1.519	1.516
C_6-C_7, C_8-C_9	1.417	1.417
C_7-C_8	1.411	1.413
Valence Angles (deg)		
$C_2-C_3-C_6, C_5-C_4-C_9$	103.5	102.4
$C_2-C_3-C_4, C_5-C_4-C_3$	107.5	107.4
$C_6-C_3-C_4, C_9-C_4-C_3$	102.3	102.2
$N_1-C_2-C_3, N_1-C_5-C_4$	107.2	107.4
$C_2-N_1-C_5$	110.6	110.4
$C_3-C_6-C_7, C_4-C_9-C_8$	97.8	93.6
$C_3-C_6-C_{10}, C_4-C_9-C_{10}$	89.0	92.2
$C_7-C_6-C_{10}, C_8-C_9-C_{10}$	107.2	106.9
$C_6-C_7-C_8, C_7-C_8-C_9$	108.9	108.9
$C_6-C_{10}-C_9$	100.1	100.5
heat of formation (kJ mol^{-1})	70.4	71.0

[a] See Figure 3 for the definition of the atoms.

geometrical changes are those corresponding to the bond lengths: the C_6-C_7, C_8-C_9, and C_3-C_4 bond lengths have increased (by about 0.5–0.7 Å in comparison with those calculated for cyclopentadiene and maleimide, Table 5) whereas a shortening of the C_7-C_8 bond length is observed (~1.41 Å versus ~1.46 Å in cyclopentadiene). These structural features are characteristic of an early transition state and result from the large exothermicity of the cycloaddition reaction. The sizeable opening of the $C_3-C_6-C_7$ and $C_4-C_9-C_8$ angles by more than 4° on going from (X) TS_c to (N) TS_c is probably indicative that the endo transition state has adjusted itself to some steric requirements.

With respect to energetical considerations, the two concerted transition states are nearly identical with a probably negligible preference for the endo transition state. The two cyclization processes are very close in energy: $\Delta_r H^{o\ddagger}$ = 79.0 kJ mol^{-1} (endo process, Table 6), $\Delta_r H^{o\ddagger}$ = 79.6 kJ mol^{-1} (exo process, Table 7). By contrast, the decyclization activation enthalpies are significantly different: 207.7 kJ mol^{-1} for the endo adduct (Table 6) versus 234.3 kJ mol^{-1} for the exo adduct (Table 7).

(b) Stepwise Pathways. As inferred by energetical data from Table 6, the most economical and shortest pathway toward the (N) adduct can be defined as first passing through a (N) transition state of TS_{ag} type lying 74.7 kJ mol^{-1} above the reactants. Further strengthening of the forming C_4-C_9 bond brings the system to the biradical structure (N) M_{ag} 85.8 kJ mol^{-1} below (N) TS_{ag}. Next, a rotation around the C_4-C_9 bond leads to the ring closure precursor (N) M_{sg} structure over a small barrier (7.6 kJ mol^{-1}, transition state: R_3). The final collapse to *endo*-nadimide which involves the (N) TS_d transition state, is achieved with an energy excess of only 21.8 kJ mol^{-1}.

Concerning the reverse process, it appears that the nonconcerted decomposition of *endo*-nadimide occurs via two stable biradical intermediates in three kinetically distinct steps controlled successively by the (N) TS_d, R_3 and (N) TS_{ag} transition states. With a 203.4 kJ mol^{-1} barrier the third step is rate determining. ORTEP plots of the two transition states (N) TS_{ag} and (N) TS_d are illustrated in Figures 4a and 5a. Complete geometrical characteristics are available on request in the form of supporting information.

Results from Table 7 bear the indication that the most economical and shortest nonconcerted route from the reactants to the (X) adduct reaches a first energy maximum which occurs for an (X) transition state of TS_t type. The corresponding activation enthalpy is 74.2 kJ mol^{-1}. From this point, a descending path leads to the biradical structure (X) M_t lying 84.6 kJ mol^{-1} below. Next, through a facile rotational process involving R_1 as a transition state ($\Delta_r H^{o\ddagger}$ = 10.3 kJ mol^{-1}) the biradical minimum (X) M_{sg} is obtained which serves as a starting point for the formation of the second Diels–Alder C–C bond. The final ring closure to *exo*-nadimide proceeds via the transition state (X) TS_d and only requires an energy excess of 20.3 kJ mol^{-1}.

With respect to the reverse process, the nonconcerted decomposition of *exo*-nadimide is found to occur via two biradical intermediates in three kinetically distinct steps controlled successively by the (X) TS_d, R_1 and (X) TS_t transition states. The latter is identified as the rate-determining transition state ($\Delta_r H^{o\ddagger}$ = 228.9 kJ mol^{-1}). ORTEP plots for (X) TS_t and (X) TS_d are represented in Figures 4b and 5b. Complete geometrical parameters are available on request in the form of supporting information.

(3) Mechanism of Isomerization of *endo*-Nadimide via a Cycloelimination–Cycloaddition Route. The breaking of one Diels–Alder C–C bond in *endo*-nadimide is calculated to be 63.8 kJ mol^{-1} less expensive than the concerted cleavage of both the Diels–Alder C–C bonds (Table 6).

An outcome of this result is a possible dependance on temperature for the mechanism of decyclization of *endo*-nadimide. At moderate temperatures, the stepwise mechanism is probably operative leading to the formation of a biradical species (N) M_{sg} with the two cyclic moieties in syn-gauche conformation and more stable than the entrance transition state by 21.8 kJ mol^{-1}. (N) M_{sg} may participate in a rotational process along which it is converted into nearly isoenergetic trans and anti-gauche conformations. The spread between the corresponding barriers being small (3.1–15.3 kJ mol^{-1}), these conformations are equally probable. The direct conversion, i.e. without scission of the remaining Diels–Alder bond, of a biradical species into *exo*-nadimide requires an hydrogen atom transfer. This possibility will be examined in the next section. In the absence of such a mechanism and unless a large excess of energy is available the biradical species recyclize to yield the initial endo adduct.

At elevated temperatures, the mechanism may be concerted or stepwise and involves the cleavage of the two Diels–Alder C–C bonds. To have a concerted retro Diels–Alder reaction, appropriate thermal conditions must be fulfilled in such a way that at least the quantity of energy necessary to cross over the TS_c transition state ($\Delta_r H^{o\ddagger}$ = 207.7 kJ mol^{-1}) is available. In the nonconcerted route, the cleavage of the first Diels–Alder bond requires 143.9 kJ mol^{-1}. For the scission of the second Diels–Alder bond via the TS_{ag} transition state an additional amount of energy of 59.5 kJ mol^{-1} is needed. Owing to the small difference (~4.3 kJ mol^{-1}) between their activation enthalpies, both concerted and stepwise processes are probably competitive at high temperature.

Our results show that formation of endo adduct and exo adduct from the regenerated addends cyclopentadi-

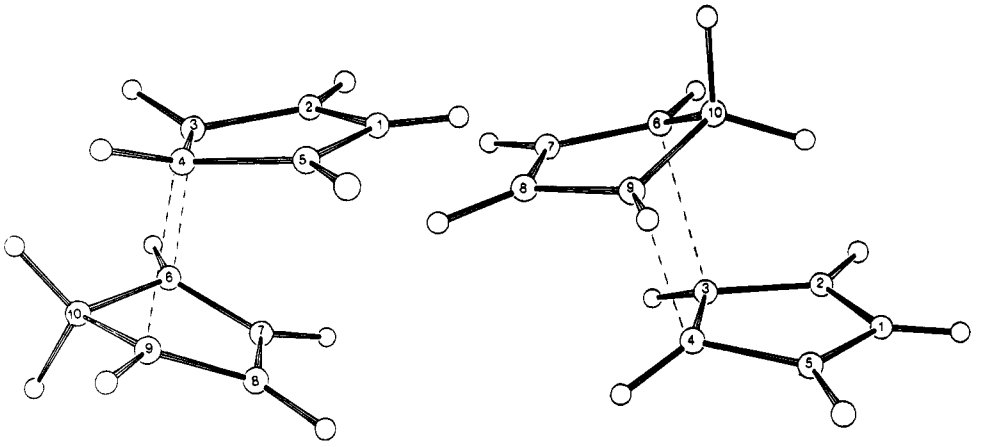

Figure 3. Diels–Alder reaction between cyclopentadiene and maleimide: ORTEP plots of the AM1-HE-SDCI optimized geometries of the concerted transition states.

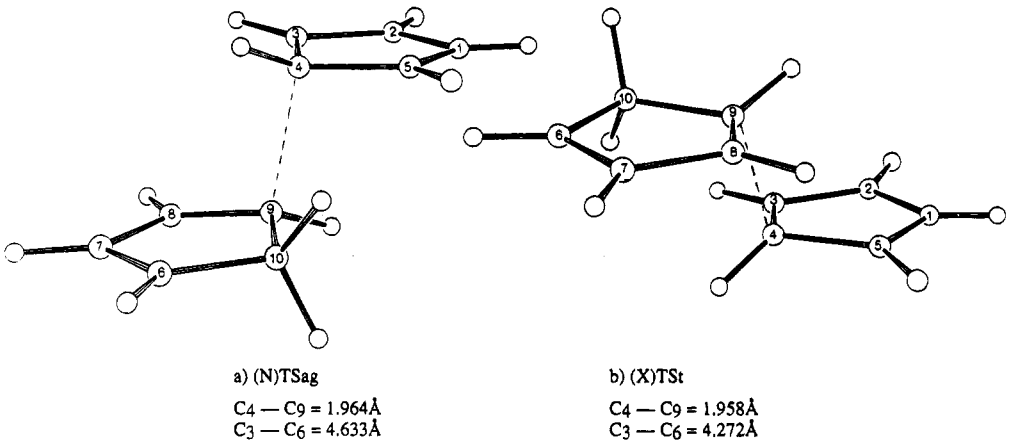

Figure 4. Diels–Alder reaction between cyclopentadiene and maleimide: ORTEP plots of the AM1-HE-SDCI optimized geometries of the one-bond rate-determining transition states.

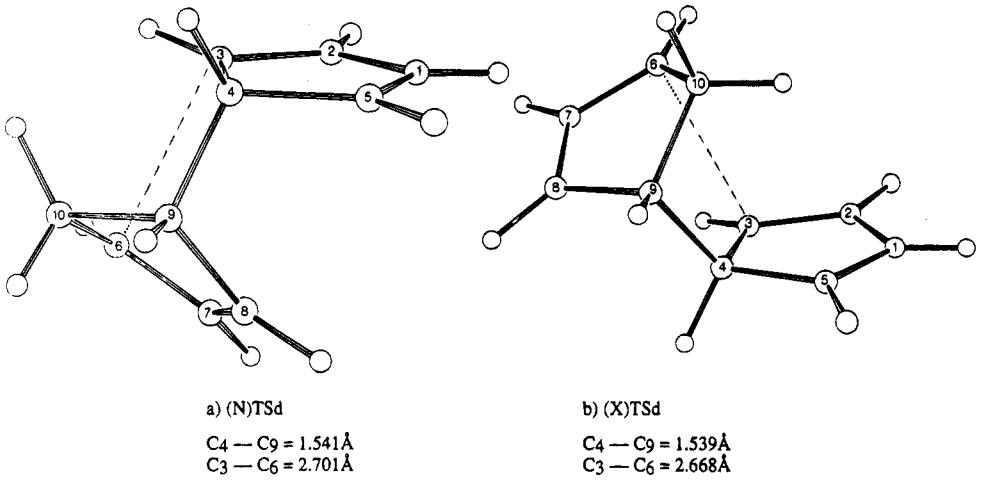

Figure 5. Diels–Alder reaction between cyclopentadiene and maleimide: ORTEP plots of the AM1-HE-SDCI optimized geometries of the lowest one-bond transition states.

ene and maleimide are nearly equally probable. The concerted processes require, respectively, 79.0 and 79.6 kJ mol^{-1}, the stepwise processes 74.7 and 74.2 kJ mol^{-1}.

(4) Isomerization of *endo*-Nadimide via an Internal Pathway Involving a Hydrogen Atom Transfer. As an alternative to the previously described decomposition–recombination sequence, nondissociative schemes have been discussed in literature.[10] In particular, the relevant question appears to be how an internal process such as intramolecular hydrogen atom transfer may contribute to the overall endo → exo conversion. In the following, we take advantage of the recently established suitability of AM1 in modeling this kind of rearrangement[23e,25,26] to test Craig's hypothesis.[10e]

After the rupture of the C_3–C_6 bond in the endo adduct the biradical species (N) M_{sg} (Figure 6) is reached which

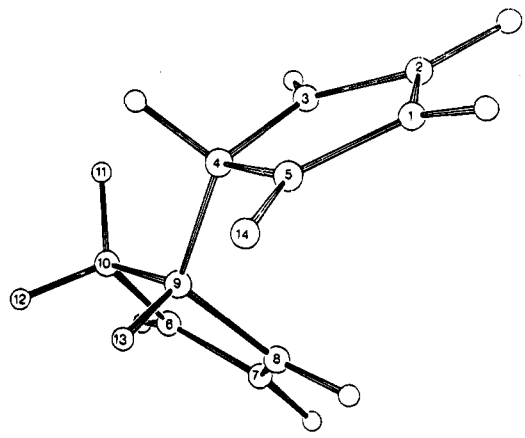

Figure 6. ORTEP plot of the AM1-HE-SDCI optimized geometry for the biradical intermediate (N)Msg.

can serve as the starting point for this intramolecular rearrangement. Depending on (i) whether hydrogen abstraction is by carbon or oxygen; (ii) whether the reaction proceeds via a stepwise or a concerted pathway. Several mechanisms are conceivable. Some of them have been investigated. The most interesting geometrical parameters of the relevant transition state structures and the corresponding energetical data are displayed in Table 9.

(a) One-Step Pathways. Migration of H_{11} or H_{12} from C_{10} to C_8 (Figure 6) is a way to convert (N) M_{sg} to the enantiomeric form of (X) M_{sg} and thus to achieve the epimerization of the endo adduct to the exo isomer. Of the two a priori possible processes, antarafacial and suprafacial, the former is unrealizable due probably to steric hindrance factors. When the migrating H_{11} atom is passed from the top face to the bottom face of the $C_{10}-C_9-C_8$ plane, very unfavorable constraints are imposed on the cyclopentadiene skeleton so that, despite extensive searches, no transition state could be located. On the other hand, suprafacial [1,3] shift of H_{12} is accessible. The results in literature support the conclusion that the rate of an intramolecular rearrangement depends to some extent on geometrical parameters such as the distances and angle of transfer between the reacting moieties.[23e,25,26,44,45] As a probable consequence of an abnormally long $C_{10}-H_{12}$ breaking bond and a severe distortion of the $C_{10}-H_{12}-C_8$ angle from the linearity, the suprafacial hydrogen migration proceeds with a very high activation enthalpy which is of the same order of magnitude as the C–H bond dissociation energy ($\Delta_r H^{\circ\ddagger}$ = 263.9 kJ mol^{-1}, Table 9).

(b) Two-Step Pathways. An alternative for the conversion of (N) M_{sg} to the enantiomeric form of (X) M_{sg} would be a sequence of two consecutive shifts involving either H_{13} next H_{12} or H_{11} alone.

(i) Processes Involving Abstracting Carbon Atoms. [1,2] Hydrogen Shifts. The shortest route connecting (N) M_{sg} and the enantiomeric form of (X) M_{sg} can be depicted as follows: C_9 and C_8 are, respectively, the first hydrogen atom source (H_{13}) and acceptor in the rearrangement. At the conclusion of this step a structure corresponding to a local minimum is reached with two radical centers at C_9 and C_3 ($\Delta_f H^\circ$ = −107.6 kJ mol^{-1}). Next, H_{12} is transferred from C_{10} to C_9. Both transition states lie about 69 kJ mol^{-1} lower in energy than the transition state calculated for the suprafacial [1,3] hydrogen transfer (Table 9).

[1,4] Hydrogen Shifts. First, a +60° rotation around the C_4-C_9 bond brings H_{11} closer to the radical center C_3. Then, a transition state is attained in which the forming C_3-H_{11} bond is nearly in the $C_{10}-C_9-C_4-C_3$ plane ($C_{10}-C_9-C_4-C_3$ = 1.5°, $H_{11}-C_3-C_4-C_9$ = 7.5°). Next, a −60° rotation leaves H_{11} bonded to C_3, and a very stable cyclopentadiene substituted succinimide is obtained ($\Delta_f H^\circ$ = −184.2 kJ mol^{-1}).

This transfer proceeds with a low activation enthalpy ($\Delta_r H^{\circ\ddagger}$ = 48.7 kJ mol^{-1}). The calculated barrier is in reasonable agreement with experimental and theoretical values for the Barton reaction.[23e,25,45a-c]

Hydrogen atom transfer reaches completion through a second step requiring the simultaneous −60° rotation around the C_4-C_9 bond, cleavage of the C_3-H_{11} bond, and formation of the C_8-H_{11} bond.

Both transition states are close energetically. They lie about 145.4–157.5 kJ mol^{-1} lower than the transition states calculated for the [1,2] hydrogen shift sequence.

(ii) Processes Involving Abstracting Oxygen Atom. A two-step mechanism for endo → exo isomerization may be envisaged in which O_{14} (Figure 6) participates as an hydrogen acceptor. Free rotation occurs and reduces the interatomic distance between H_{11} and the abstracting heteroatom, H_{11} is transferred, and a minimum intermediate is obtained ($\Delta_f H^\circ$ = −107.6 kJ mol^{-1}). In a similar fashion, migration of H_{11} between O_{14} and C_8 converts this minimum into one of the exo biradical species. For processes involving O_{14} the degree of strain in the transition structures seems to be comparable to that observed in theoretical models of MacLafferty and Norish type intramolecular rearrangements:[26,45c-e] in particular, the angles of transfer α come closer to 180° (Table 9). However, the calculated barriers, 229.9 kJ mol^{-1} for the first step and 151.1 kJ mol^{-1} for the second step, are greater than the typically low or nonexistent experimental barriers.[26,46]

(c) Most Probable Mechanism for Isomerization by Intramolecular Hydrogen Atom Transfer. As stated above a conformationally mobile biradical species (N) M_{sg} is probably formed at moderate temperature. It appears that the best way to achieve isomerization without retrogression to the addends involves a two-step [1,4] shift of hydrogen atom. The first step, which requires a small amount of energy (48.7 kJ mol^{-1}), leads to a very stable succinimide type species ($\Delta_f H^\circ$ = −184.2 kJ mol^{-1} to be compared with $\Delta_f H^\circ$ = −15.2 kJ mol^{-1} for (N) M_{sg}). This prediction is in line with experimental studies showing the production of significant quantities of N-substituted succinimides in the Diels–Alder reactions of N-substituted nadimides.[3,8] In the second step, an exo biradical species is reached via a transition state which is lower in energy than that involved in the first step ($\Delta_f H^\circ$ = 22.1 kJ mol^{-1} versus 33.5 kJ mol^{-1}).

(44) Green, M. M.; Boyle, B. A.; Vairamani, M.; Mukhopadhyay, T.; Saunders, W. H., Jr.; Bowen, P.; Allinger, N. L. *J. Am. Chem. Soc.* **1986**, *108*, 2381. Djerassi, C.; Von Mutzenbecher, G.; Fajkos, J.; Williams, D. H.; Budzikiewicz, H. *J. Am. Chem. Soc.* **1965**, *87*, 817. Brun, P.; Waegell, B. *Reactive intermediates*; Plenum Press: New York, 1983; Vol. 3, p 367 and references therein. Bingham, R. C.; Dewar, M. J. S. *J. Am. Chem. Soc.* **1972**, *94*, 9107.

(45) (a) Dorigo, A. E.; Houk, K. N. *J. Am. Chem. Soc.* **1987**, *109*, 2195. (b) Dorigo, A. E.; Houk, K. N. *J. Org. Chem.* **1988**, *53*, 1650 and references therein. (c) Dorigo, A. E.; Mac Carrick, M. A.; Loncharich, R. J.; Houk, K. N. *J. Am. Chem. Soc.* **1990**, *112*, 7508. (d) Liu, R.; Pulay, P. *J. Comput. Chem.* **1992**, *13*, 183. (e) Boer, F. P.; Shannon, T. W.; MacLafferty, F. W. *J. Am. Chem. Soc.* **1968**, *90*, 7239.

(46) Kingston, D. G. I.; Bursey, J. T.; Bursey, M. M. *Chem. Rev.* **1974**, *74*, 215 and references therein.

Table 9. Enthalpies and Structural Features of the Transition States for Internal Hydrogen Atom Transfers from Atom X (carbon or oxygen) to Atom Y (carbon or oxygen) in the Biradical Intermediate (N) M_{sg} (distances in angströms, angles in degrees)

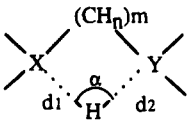

Mi → TS → Mj

n = 0, 1, 2, 3

X[a]	Y[a]	m	hydrogen atom transferred	geometrical parameters of the transition state d_1	d_2	α	enthalpy of formation of the transition state (kJ mol^{-1})	$\Delta_r H^{\ddagger}_{Mi\rightarrow Mj}$ (kJ mol^{-1})	$\Delta_r H^{\ddagger}_{Mj\rightarrow Mi}$ (kJ mol^{-1})
C_{10}	C_8	1	H_{12}	1.887	3.246	46.1	248.7	263.9	265.9
C_9	C_8	0	H_{13}	1.385	1.369	64.5	179.6	194.8	287.2
C_{10}	C_9	0	H_{12}	1.307	1.387	64.4	178.9	286.5	196.2
C_{10}	C_3	2	H_{11}	1.220	1.600	120.8	33.5	48.7	217.7
C_3	C_8	2	H_{11}	1.603	1.222	123.0	22.1	206.3	39.3
C_{10}	O_{14}	3	H_{11}	1.433	1.222	143.9	214.7	229.9	156.0
O_{14}	C_8	3	H_{11}	1.432	1.222	146.7	209.8	151.1	227.0

[a] See Figure 6 for the definition of the atoms.

As a consequence, the reaction may bypass this succinimide intermediate. The ultimate collapse of the (X) M_{sg} intermediate to form the exo adduct requires an amount of energy of only 20.3 kJ mol^{-1} ($\Delta_f H°$ (TS_d) − $\Delta_f H°$ (M_{sg}), cf. Table 7).

It arises from these results that even at moderate temperature endo → exo isomerization of nadimide may occur through an intramolecular hydrogen atom transfer. At elevated temperature, the isomerization process probably traverses the other mechanistic pathway, i.e. the cycloelimination−cycloaddition route.

(5) Comparison with Experimental Results in This Series. Analysis of Medium Effects. To the best of our knowledge, the only experimental kinetic studies which have been carried out in this series are those dealing with the cyclopentadiene + *N*-methyl- or *N*-phenylmaleimide systems. Moreover, only the direct Diels−Alder processes have been investigated. In dioxane the endo adduct is found to be kinetically preferred.[47] As inferred by the similarity in the experimental activation enthalpies of the two systems (respectively, 35.9 and 31.3 kJ mol^{-1}) the phenyl substituent has a minor effect on the kinetic parameters of the reaction. From this, the use of nadimide to model the reactivity of *N*-phenylnadimide is confirmed to be quite appropriate.

Theoretical data allow the prediction that formation of endo and exo adducts from cyclopentadiene and maleimide are competitive. The concerted pathways require, respectively, 79.0 and 79.6 kJ mol^{-1}, the stepwise pathways 74.7 and 74.2 kJ mol^{-1}, i.e. theoretical values which are nearly twice the experimental $\Delta_r H°^{\ddagger}$s. As mentioned above, these discrepancies may be caused by a deficiency of the AM1-HE-SDCI procedure for the description of the reactants. In addition, our theoretical $\Delta_r H°^{\ddagger}$ values which refer to the gas phase are not strictly comparable to experimental data which are obtained from solutions. Medium effects, i.e. essentially solvent polarity and internal pressure, can be held responsible, at least partly, for these differences between theory and experiment.

(a) Solvent Polarity Effect. An increase in the reaction rate with increasing solvent polarity is usually interpreted in terms of a transition state more polar than the initial state.[13e]

Aqueous solvation energies have been calculated in the framework of the AM1-SM2 model[48] (Table 10). This model includes local-field terms representing solvent electric polarization, cavity creation, dispersion interaction, and change of solvent structure. Moreover these terms are treated self-consistently with a solute electronic Hamiltonian.

Despite (i) the significant increase in the dipolar moment of the system on going from reactants to transition state and (ii) the strong polarity of water (ϵ = 80), the relative stabilities of reactants and transition states are not practically modified by solvation so that no appreciable variation of the activation barrier is found. Therefore, the rate of the reaction is probably insensitive to changes in the polarity of the solvent.

(b) Internal Pressure Effect.[13e,49] According to the theory of Eyring, the pressure dependance of the reaction rate k is expressed as:

$$\left(\frac{\partial \ln k}{\partial p}\right)_T = -\frac{\Delta V^{\ddagger}_m}{RT} \text{ (ref 50)} \qquad (2)$$

where T is the absolute temperature, p the pressure in the reaction mixture and $\Delta V^{\ddagger}_m$ the activation volume.

As reported elsewhere,[23d] even at 1 atm of external pressure the pressure within a condensed phase can be quite high. According to eq 2 large $\Delta V^{\ddagger}_m$ values may be the cause of large changes in reaction rates.

For lack of experimental data, $\Delta V^{\ddagger}_m$ can be calculated from the equation:

$$\Delta V^{\ddagger}_m = V^{\ddagger}_m - \sum_i V_{m,i} \qquad (3)$$

(47) Sauer, J.; Wiest, H.; Mielert, A. *Chem. Ber.* **1964**, *97*, 3183.

(48) Cramer, C. J.; Truhlar, D. G. *Science* **1992**, *256*, 213.

(49) (a) Asano, T.; Le Noble, W. J. *Chem. Rev.* **1978**, *78*, 407. (b) MacCabe, J. R.; Eckert, C. A. *Acc. Chem. Res.* **1974**, *7*, 251. (c) Jenner, G. *Angew. Chem., Int. Ed. Engl.* **1975**, *14*, 137. (d) Van Eldik, R.; Asano, T.; Le Noble, W. J. *Chem. Rev.* **1989**, *89*, 549. (e) Klärner, F. G.; Dogan, B. M. J.; Ermer, O.; Doering, W. Von E.; Cohen, M. P. *Angew. Chem., Int. Ed. Engl.* **1986**, *25*, 108. (f) Klärner, F. G. *Chem. Unserer Zeit.* **1989**, *23*, 53. (g) Klärner, F. G.; Ruster, V.; Zimny, B.; Hochstrate, D. *High Pressure Res.* **1991**, *7*, 133. (h) Diedrich, M. K.; Hochstrate, D.; Klärner, F. G.; Zimny, B. *Angew. Chem., Int. Ed. Engl.* **1994**, *33*, 1079. (i) Blokzijl, W.; Blandamer, M. J.; Engberts, J. B. F. N. *J. Am. Chem. Soc.* **1991**, *113*, 4241.

Table 10. Diels–Alder Reaction between Cyclopentadiene and Maleimide: Calculated Dipole Moments and Solvation Energies in Aqueous Solution for the Reactants and Transition States

	dipole moment (D)		solvation energy in aqueous solution (kJ mol^{-1})[c]
	gas phase[a]	aqueous solution[b]	
reactants			
cyclopentadiene	0.543	0.807	−2.0
maleimide	1.905	2.759	−45.7
(N) transition states			
TS_c	3.717	5.362	−46.3
TS_t	3.756	5.537	−45.1
TS_{sg}	3.925	5.911	−47.5
TS_{ag}	3.910	6.428	−41.9
(X) transition states			
TS_c	3.224	4.816	−41.9
TS_t	4.131	6.462	−43.2
TS_{sg}	3.548	5.813	−44.1
TS_{ag}	3.973	5.831	−44.7

[a] AM1 calculated dipole moment. [b] AM1-SM2 calculated dipole moment.[48] [c] AM1-SM2 solvation energy in aqueous solution.

where $V_m^{\ddagger}$ and $V_{m,i}$ are respectively the molar volume for the transition state and each reactant. Only $V_{m,i}$ values can be directly obtained from experiments. A way to a theoretical estimate of $V_m^{\ddagger}$ may be through the relation:

$$V_m^{\ddagger} = V_m^{(w)\ddagger}/\eta \text{ (ref 49h)} \qquad (4)$$

where (1) $V_m^{(w)\ddagger}$ is the molar Van der Waals volume of the transition state calculated using the AM1-HE-SDCI optimized geometry and the classical Van der Waals radii of the different atoms (r_H = 1.2 Å, r_O = 1.4 Å, $r_C = r_N$ = 1.5 Å), and (2) η is the packing coefficient for the transition state usually approximated from the packing coefficient of a stable parent system for which V_m and $V_m^{(w)}$ are accessible.

In the case of the cyclopentadiene–maleimide system, the similarity in shape between each adduct and the corresponding transition state TS_c should allow the packing coefficient to be transferred from the adduct to the TS_c transition state but, due to the lack of experimental molar volumes for both *endo*- and *exo*-nadimides, the packing coefficients in demand cannot be estimated.

For the parent cyclopentadiene–maleic anhydride system we also observed a similarity in shape between each adduct and the corresponding transition state TS_c. In that case, the experimental molar volume of the cyclopentadiene–maleic anhydride endo adduct is available[51] so that the packing coefficient can be calculated. We propose to use the packing coefficient calculated for the cyclopentadiene–maleic anhydride endo adduct to evaluate the molar volume $V_m^{\ddagger}$ of the cyclopentadiene–maleimide (N)TS_c transition state.

Experimental molar volume for the cyclopentadiene–maleic anhydride endo adduct is 115.9 cm^3 mol^{-1}.[51] The Van der Waals volume of the corresponding AM1-HE-SDCI optimized structure is 79.4 cm^3 mol^{-1}. From eq 4 we obtain η = 0.685.

For the cyclopentadiene–maleimide (N)TS_c transition state (Table 8, Figure 3a) the Van der Waals volume is 78.8 cm^3 mol^{-1}. Assuming η = 0.685, the molar volume of this transition state is estimated to be 115.0 cm^3 mol^{-1}. With V_m (cyclopentadiene) = 82.4 cm^3 mol^{-1} [52] and V_m (maleimide) = 80.5 cm^3 mol^{-1} [53] a value of $\Delta V_m^{\ddagger}$ = −47.9 cm^3 mol^{-1} is found which is in the range of experimental data for reactions involving maleic anhydride as a dienophile.[13e] This large value can explain a possible contribution of the internal pressure effect to the difference between the experimental rate measured in solution and the corresponding gas phase prediction.

For the cyclopentadiene–maleimide endo adduct a molar volume of 113.9 cm^3 mol^{-1} is calculated.[54] This leads to a $\Delta V_m^{\ddagger}$ value close to zero (113.9–115.0 cm^3 mol^{-1}) for the reaction of decomposition of the endo adduct. Here, no significant internal pressure effect is expected. It emerges from these results that our AM1 calculated decyclization barrier probably gives a good account of experimental data from both the gas phase and the solution phase.

Conclusion

The present paper provides a theoretical model of the conversion of *endo*-nadimide to its exo isomer within the AM1-HE-SDCI formalism. The eventuality of competing external (i.e. completely dissociative) and internal (i.e. partially dissociative) reaction pathways has been investigated.

Retrogression of *endo*-nadimide to the addends can be accomplished by a concerted or a stepwise process. The latter starts with the cleavage of one C–C bond leading to a stable endo biradical species and reaches completion with the scission of the second C–C bond. This last step is rate determining. At the AM1-HE-SDCI level the concerted and stepwise pathways are predicted to be nearly energetically equivalent. These results suggest that biradical intermediates may be obtainable under thermal activation and thus may initiate the homopolymerization of the norbornene rings in PMR prepolymers.

Recombination of the addends to give *exo*-nadimide is shown to proceed via a concerted route as well as a stepwise pathway involving a conformationally mobile biradical intermediate of exo type.

We have obtained quite conclusive evidence that endo → exo isomerization is possible without passing through dissociated addends. As an alternative to the cycloelimination–cycloaddition route, a sequence of two consecutive [1,4] shifts of hydrogen atom can easily transform the endo biradical intermediate into the corresponding exo biradical precursor of *exo*-nadimide.

Finally, we predict that solvent polarity and internal pressure have probably minor effects on the rate of decomposition of *endo*-nadimide. On the contrary, due probably to the large corresponding activation volume, the rate of formation of nadimide is likely pressure dependent.

Supporting Information Available: Supplementary Tables 11–13 (3 pages). This material is contained in libraries on microfiche, immediately follows this article in the microfilm version of the journal, and can be ordered from the ACS; see any current masthead page for ordering information.

JO9507294

(50) Evans, M. G.; Polanyi, M. *Trans. Faraday Soc.* **1935**, *31*, 875.
(51) Destro, R.; Filippini, G.; Gramaccioli, C. M.; Simonetta, M. *Acta Crystallogr.* **1969**, *B25*, 2465.
(52) Experimental molar volume from the Handbook of Chemistry and Physics.
(53) Estimated from the molar Van der Waals volume of the AM1-HE-SDCI optimized structure of maleimide ($V_m^{(w)}$ = 41.4 cm^3 mol^{-1}) and the packing coefficient of maleic anhydride (η = 0.514).
(54) The packing coefficient of the cyclopentadiene maleic anhydride endo adduct is used in this calculation.